
Multi-Source Domain Adaptation Using Approximate Label Matching

Jordan T. Ash

Princeton University

JORDANTASH@GMAIL.COM

Robert E. Schapire

Microsoft Research

SCHAPIRE@MICROSOFT.COM

Abstract

Domain adaptation, and transfer learning more generally, seeks to remedy the problem created when training and testing datasets are generated by different distributions. In this work, we introduce a new unsupervised domain adaptation algorithm for when there are multiple sources available to a learner. Our technique assigns a rough labeling on the target samples, then uses it to learn a transformation that aligns the two datasets before final classification. In this article we give a convenient implementation of our method, show several experiments using it, and compare it to other methods commonly used in the field.

1. Introduction

Intuitively, truly intelligent agents should be able to improve on one task after having learned a similar kind of task. A human, for example, might be more capable of speaking Italian after having learned Spanish, or of programming a computer in Java after having learned C++. The goal of domain adaptation is to endow machine learning with this same sort of behavior.

In the usual classification or regression framework, we assume that training and testing data are generated by the same underlying distribution. When this assumption does not hold, testing performance can be significantly worse than training performance.

This general problem, where training and testing datasets come from different distributions, comes up frequently in many areas of machine learning, especially Natural Language Processing (NLP) (Jiang & Zhai, 2007; Glorot et al., 2011) and computer vision (Beijbom, 2012; Patel et al.,

2015).

Our work was motivated by a problem arising in the classification of magnetoencephalography (MEG) data. MEG machines use magnetic fields to measure the brain's electrical activity, and are frequently used for experiments in neuroscience and psychology. In the specific problem we consider, which was originally part of an online competition, data came from sixteen different people who were shown either pictures of human faces or non-faces (images with no discernible face-like structures), and had their brain activities recorded using MEG. The goal of this challenge was to classify instances where the subject was looking at a face from those where the subject was not. Figure 1 shows this data embedded into two dimensions using t-distributed stochastic neighbor embedding (t-SNE) (van der Maaten & Hinton, 2008).

In Figure 1, each cluster of points, or domain, corresponds to data generated by a different subject. This is a clear domain adaptation problem because, while each of the training subject datasets appear easily classifiable, none of their hypotheses would obviously transfer well to the held-out data.

Still, each subject's data appears to be rotated and translated with respect to most other subject's data. If we want to transfer a classification hypothesis from one subject's data, which we will refer to as a source, to a held-out subject, which we will refer to as a target, it would be sufficient to find a transformation that aligns these two datasets. The goal of our technique, and others like it, is to uncover such a transformation. Because we are not provided in our training set with any labeled samples that are generated by the distribution that generates the target data, the problem is called unsupervised.

In this work we present a new method for unsupervised domain adaptation. Our approach assigns an approximate, better-than-guessing labeling to the target dataset, then uses this labeling to uncover a transformation that matches the target data with the data from a particular source.

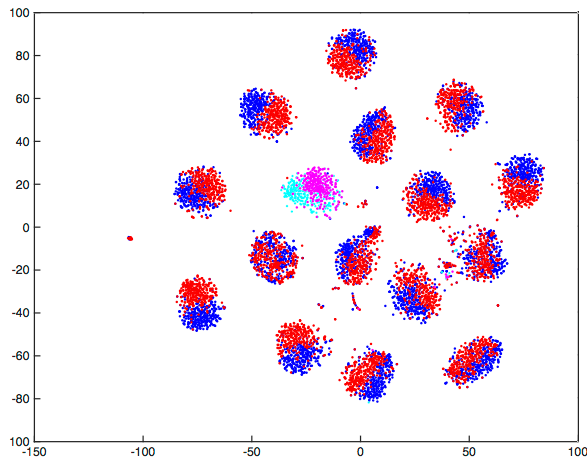


Figure 1. A two-dimensional t-SNE embedding of the MEG data. Red and Blue correspond to negative and positive source samples, while magenta and cyan correspond to negative and positive samples for a held-out target. In our framework, a learner does not have access to any labels from the target dataset

After describing the technique in detail, we will provide illustrative and practical examples demonstrating its performance in several spheres.

1.1. Related Work

As described in (Mohri, 2015), domain adaptation has historically been approached in mainly two ways.

In one, training samples are re-weighted to make the resulting hypothesis better suited to classification on the testing set. Kernel Mean Matching (KMM) is a well-known domain adaptation technique that falls into this category (Gretton et al., 2009). This algorithm re-weights source points in an effort to make the means of the source and target dataset as close as possible in a reproducing kernel Hilbert space. An advantage of KMM is that it circumvents the need to approximate any distributions.

In the alternative approach, the source and/or target datasets are transformed into a different space where they better match each other. Transfer Component Analysis (TCA) operates in this way (Pan et al., 2011), attempting to find a set of “transfer components” such that source and target datasets appear to have the same underlying distribution when projected into this new space.

Because we attempt to transform the target data to make it look like the source data, our method falls into the latter category.

2. Our Method

2.1. Problem Setup

In our problem, the learner has been given k source datasets $(X_1^s, Y_1^s), \dots, (X_k^s, Y_k^s)$ from which it tries to transfer knowledge, and one target sequence $X^t = \langle x_1^t, \dots, x_n^t \rangle$ to which it tries to transfer knowledge. Each source dataset (X_i^s, Y_i^s) is composed of sequences $X_i^s = \langle x_{1,i}^s, \dots, x_{m_i,i}^s \rangle$ and $Y_i^s = \langle y_{1,i}^s, \dots, y_{m_i,i}^s \rangle$. Every $y_j^s \in \{-1, 1\}$ corresponds to a label on $x_j^s \in \mathbb{R}^d$. For each $x_j^t \in \mathbb{R}^d$ in the target sequence, the goal of the classifier is to assign a label $y_i^t \in \{-1, 1\}$ for each target example x_i^t .

We assume that within each source i , each labeled example $(x_{i,j}^s, y_{i,j}^s)$ is generated according to the same distribution, and likewise for the target. However, the distributions associated with the various sources and the target will generally all be different, although we think of them as being similar enough for learning to be transferred, to some degree, from one to another.

A sentiment classification model trained on a corpus of book reviews, for example, may generalize poorly when reviews are considered from the domain of kitchen appliances. Similarly, a classifier that is trained on MEG data from one person may generalize poorly when used on data generated by another person that might have a different skull geometry, apparatus alignment, or neurological physiology.

One natural solution to this classification problem is to combine all the source datasets (X_i^s, Y_i^s) , so that we can a model, which we call g , on all available sources simultaneously. Of course, because the testing data X^t is generated from a distribution that may be unlike any of those composing the training set, we expect this hypothesis might not work very well. In many cases though, g might not be terrible, and so we assume that it is, at a minimum, better than random guessing on the target data.

Another natural solution might be to treat each X_i^s as a separate training set. In this framework, we would have k separate “local” classifiers, which we refer to as f_i . Again, as Figure 1 shows, because X^t is generated from a different distribution from any of the X_i^s , we cannot expect any particular f_i to perform as well on samples from X^t as it does on samples from X_i^s . Once each f_i has been trained, the learner has access to k different labelings on each of the samples in X^t , and a classification for a target sample $x_j^t \in X^t$ can be returned as $\text{sign}(\sum_{i=1}^k f_i(x_j^t))$.

Again, in Figure 1, every domain appears to be rotated and translated with respect to every other domain. Motivated by such situations, we suppose that each source domain (X_i^s, Y_i^s) can be transformed to “look like” a target domain via a transformation ϕ_i . Even though each f_i probably will

Algorithm 1 Approximate Label Matching

Input: $(X_1^s, Y_1^s), \dots, (X_k^s, Y_k^s)$ and X^t
 $X^s \leftarrow \text{concat}(X_1^s, \dots, X_k^s)$
 $Y^s \leftarrow \text{concat}(Y_1^s, \dots, Y_k^s)$
 $g \leftarrow \text{train}(X^s, Y^s)$
for $i = 1, 2, \dots, k$ **do**
 $f_i \leftarrow \text{train}(X_i^s, Y_i^s)$
 $\phi_i \leftarrow \arg \min_{\phi_i} \left\{ \sum_{j=1}^n (g(x_j^t) - f_i(\phi_i(x_j^t)))^2 \right\}$
end for
return $\text{sign}\{\sum_{i=1}^k f_i(\phi_i(x_j^t))\}$

not transfer well on average to a fixed sample x_j^t , it hopefully will transfer well to $\phi_i(x_j^t)$. So, if we can find an appropriate ϕ_i for each available source, we can assign a reasonable final hypothesis for each target sample as

$$\text{sign}\left(\sum_{i=1}^k f_i(\phi_i(x_j^t))\right). \quad (1)$$

In order to uncover these transformations, we leverage our assumption that g performs better than guessing on the target data. We use the output of g on the samples in X^t as an approximate labeling that allows us to solve for ϕ_i . Specifically, we are interested in the ϕ_i that minimizes the difference between $g(x_j^t)$, our rough labeling, and $f_i(\phi_i(x_j^t))$ on average. We can attempt to find such a transformation ϕ by minimizing the squared error between these two different labelings of x_j^t , that is, by minimizing:

$$\sum_{j=1}^n (g(x_j^t) - f_i(\phi_i(x_j^t)))^2 \quad (2)$$

The intuitive idea is that f_i is the correct decision boundary shape, and we only need to find a way to align X_t to X_s^i in order for f_i to transfer well. Because $g(x_j^t)$ produces a labeling that is better than guessing, the best ϕ_i hopefully occurs when $g(x_j^t)$ and $f_i(\phi_i(x_j^t))$ agree most.

This classification procedure as a whole is summarized by Algorithm 1. Here, $\text{train}(X, Y)$ trains a model on dataset (X, Y) and $\text{concat}(X_1, \dots, X_k)$ concatenates sequences X_1 through X_k . To find ϕ_i for a fixed source i , we first train classifiers g and f_i , and then solve for ϕ_i by minimizing Equation (2). Once we have done this procedure for all available sources, we return a consensus labeling according to Equation (1).

2.2. Implementation

These ideas can be implemented using a neural network. Specifically, we make each f_i a neural network of arbitrary

architecture, and then use it to learn ϕ_i . As a reminder, by the time we are solving for ϕ_i , f_i and g have already been trained and are fixed. To find ϕ_i for source i , we simply take the already-trained f_i neural network and add one or more additional layers before its existing input layer.

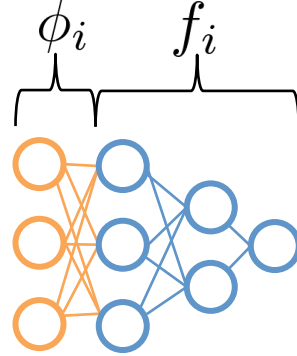


Figure 2. A diagram of our implementation with one additional layer added for ϕ . Nodes and weights in blue correspond to f_i , and those in orange correspond to ϕ_i .

These additional layers are connected to f_i by linear neurons and represent ϕ_i . When training this aggregate network, we use $g(x_j^t)$ as labels on x_j^t for back-propagation, and we do not update any of the weights in the layers corresponding to f_i . This implementation is convenient because it allows us to easily optimize (2) even though ϕ_i is nested in f_i .

It is worth mentioning that this same basic method can be used even when we are interested in transformations of a particular class. For example, to constrain ϕ_i to the space of rotation matrices, we have been able to leverage a solution to Wahba’s problem (Markley, 1988) at every iteration of back propagation.

2.3. An Illustration

Now we show a synthetic example to provide further insight into our algorithm. In this illustration, we generate a sine wave as the correct dichotomizer between positives and negatives. We then create five sources centered at different random locations along the sine wave. Each source consists of a thousand points, which are labeled as positive if they fall above the sine wave and negative otherwise. Figure 3 shows an example of this scenario.

For this illustration g is logistic regression and each f_i is a neural network with a single hidden layer composed of three hidden nodes. A randomly-chosen domain is held out as a target, and we attempt to assign labels to it by transferring knowledge from the four remaining labeled domains.

By looking at Figure 3, it is clear that g , trained on four

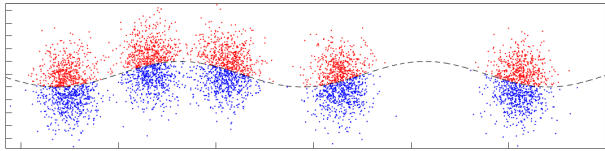


Figure 3. An example of five randomly generated domains

sources simultaneously, will be able to classify any held-out domain fairly well. However, because the correct decision boundary is sinusoidal and curved, the linear hypotheses learned by g will be less than optimal.

Similarly, f_i , which is trained on only one source, may or may not classify a held out target well. Instead of applying f_i or g to classify the target directly, we use them to learn a transformation ϕ_i that makes our target data align to a particular source. By following this process for all sources we could finally output a classification according to Equation (1).

After running this experiment a hundred times, we find that $g(x_j^t)$, $f_i(x_j^t)$, and $f_i(\phi_i(x_j^t))$ have average error fractions of .16, .08, and .07 on held-out domains. These particular numbers are not very important, and certainly vary with experimental parameters that define the sine wave and source distributions. Still, it is notable that the average $f_i(\phi_i(x_j^t))$ is able to outperform the two naive methods of classification.

3. Experiments

3.1. Experimental Setting

This section describes three separate experiments that were conducted with our technique. For each experiment, we add one additional layer to f_i when solving for ϕ , restricting ϕ to a linear transformation. In each subsection, we report different error rates for each available domain. This is done by holding out a fixed domain as a target, then using every other domain as a labeled source. For a comparison, we also include error rates for the two natural hypotheses described earlier, $g(x_j^t)$ and $\text{sign}(\sum_{i=1}^k f_i(x_j^t))$, as well as those resulting from TCA and KMM.

The TCA (Pan et al., 2011) algorithm takes a source and target as inputs and returns a canonical feature representation. Once in this space, a neural network with the same architecture as g and each f_i is used for classification.

KMM (Gretton et al., 2009) also takes a source and target as inputs, and produces a set of weights corresponding to the importance of classifying each source instance correctly. These weights were then normalized, and a training set was constructed by sampling instances of the source

dataset with replacement from the resulting distribution. Again, this training set was used to train a neural network with the same architecture as g and f_i .

TCA and KMM both allow the user to choose a kernel. In these experiments, we found that both worked best when used with a radial basis function.

Because TCA and KMM are both able to transfer knowledge from a single source to a single target, the reported errors are for labelings that result from aggregating the confidence-weighted vote of the classification scores produced from each individual source.

We also report the results of a “cheating” experiment, in which a learner is asked to classify some samples from the target data after being given labeled samples from the same domain. This classifier is again a neural network with the same architecture as f_i and these errors are computed using ten-fold cross validation. The purpose of this is to show for comparison how well the learner can do in a setting in which training and testing examples come from the same distribution

3.2. MEG data

The MEG dataset was provided by Kaggle, a data science competition website, in a challenge sponsored by several companies, including Elekta Oy, MEG International Services, Fondazione, and Besa. The features of this data are derived by estimating each subject’s covariance matrix (Barachant & Congedo, 2014) and then computing a vector according to (Barachant et al., 2013). This representation, when projected down into two dimensions, is what is shown in Figure 1. As stated earlier, labels correspond to whether or not the subject was looking at a face at the time the MEG data was recorded.

For this challenge, g and f_i are both neural networks with a single hidden layer composed of ten nodes. There are 16 different subjects available in this dataset, each containing an average of 588 samples, and errors corresponding to experiments holding out each are outlined in Table 1.

Figure 4 shows our method in action. For visualization purposes, we project dimensionality to two by using t-SNE on the source and target separately before learning ϕ_i . Before the transformation, the two datasets together seem chaotic and randomly labeled, but after transforming the target, the datasets appear orderly and easily classifiable.

3.3. Sentiment Classification

In the sentiment dataset, we are provided with product reviews from Amazon.com (Blitzer et al., 2007). Each review comes from either Amazon’s book, DVD, electronics, or kitchen department, and each of these domains contains

Table 1. A breakdown of error percentage for each domain. The final line in the table is the mean error.

	CHEAT	$g(x_j^t)$	$f_i(x_j^t)$	ALM	TCA	KMM
1	14.4	25.9	58.7	20.0	19.8	28.1
2	19.3	37.8	65.7	32.5	36.1	31.9
3	18.4	39.6	49.6	33.0	39.7	35.9
4	7.6	29.1	58.7	13.6	32.3	17.8
5	9.3	33.1	28.5	23.0	30.3	29.5
6	15.3	36.7	44.9	19.0	29.9	31.4
7	11.7	37.2	34.0	16.8	40.8	23.4
8	8.9	38.8	24.4	20.6	29.2	29.7
9	10.5	30.1	41.5	14.8	28.2	20.0
10	14.7	31.8	30.1	17.8	26.2	23.9
11	25.4	34.9	58.9	30.4	31.0	32.7
12	12.4	24.4	68.2	16.5	29.6	25.2
13	16.0	32.3	36.3	21.4	34.6	28.7
14	8.9	30.2	18.8	14.8	25.0	18.3
15	7.7	29.8	15.6	19.8	30.1	31.9
16	9.4	44.5	28.1	30.0	37.4	36.1
	13.1	30.7	41.3	21.5	31.3	27.8

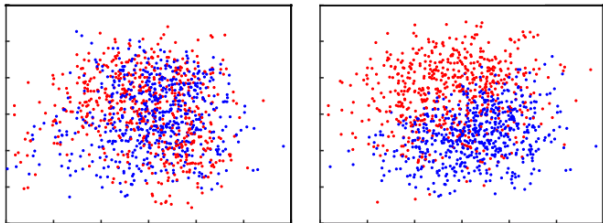


Figure 4. A source (subject 16) and target (subject 1) from the MEG dataset before learning ϕ_i (left) and after being transformed by ϕ_i (right). Positive and negative samples are colored in blue and red respectively, but only labels on the source are available to the learner.

2,000 samples. Reviews are supplied as term frequencies, which we converted into a TF-IDF representation. We then performed Principal Components Analysis (PCA) on the entire dataset, capturing 95% of its total variance and dramatically reducing its dimensionality.

In this experiment g and f_i have the same architecture as in the MEG experiment, but with a hundred hidden nodes each instead of ten. As in the previous experiment, Table 2 shows a breakdown of percent errors. Our approach achieves lower classification errors than any of the competing methods used.

3.4. Remote Sensing

The remote sensing data is created from samples produced when trying to detect landmines. Here, samples are nine-dimensional representations of radar signals. This dataset

Table 2. Errors for the sentiment classification task.

	CHEAT	$g(x_j^t)$	$f_i(x_j^t)$	ALM	TCA	KMM
B	18.7	22.4	21.5	19.8	21.3	32.3
D	16.9	20.7	20.5	18.9	22.6	29.5
E	15.8	19.0	18.2	17.2	18.4	25.1
K	13.3	16.1	15.0	13.5	16.6	24.5
	16.1	19.5	20.4	17.3	19.7	27.8

has 29 different domains, where each is affiliated with different geographical conditions. The labels represent whether or not a particular sample corresponds to the existence of a landmine. Each domain contains about 511 samples on average and, unlike in the previous two experiments where classes were balanced, there are about 15 negative samples for every positive sample. More information about this data can be found in (Xue et al., 2007).

In this experiment, g and f_i both have a single hidden layer with five neurons. Detailed results can be found in 3. In this experiment, our method performs a bit worse on average than TCA.

4. Discussion

While our technique appears to work well in each of the experiments, it particularly excels, compared to other approaches, on the MEG and sentiment classification tasks. In the MEG experiment, our approach outperforms other classification algorithms in 12 of the 16 domains. It also performs significantly better on average than both g and f_i .

In the sentiment classification problem, our approach produces hypotheses that are superior to other approaches across all domains.

The method is less successful on the landmine dataset. This is probably because KMM and TCA only consider samples from the source and target, rather than using both samples and labels. While this appears to be a disadvantage in the other two experiments, where classes are well-balanced, it seems to be an advantage in this case because there are far more negative samples than positive samples.

References

- Barachant, A. and Congedo, M. A plug & play P300 BCI using information geometry. *arXiv preprint arXiv:1409.0107*, 2014.
- Barachant, A., Bonnet, S., Congedo, M., and Jutten, C. Classification of covariance matrices using a Riemannian-based kernel for BCI applications. *Neurocomputing*, 112:172–178, 2013.

Table 3. Error percentages across domains in the remote sensing data

	CHEAT	$g(x_j^t)$	$f_i(x_j^t)$	ALM	TCA	KMM
1	8.2	8.8	21.3	6.9	6.0	23.1
2	8.4	7.8	19.5	7.9	7.3	22.8
3	8.4	7.1	15.9	6.6	6.0	18.8
4	8.2	6.2	10.2	7.4	4.1	11.0
5	8.3	5.1	6.4	6.2	4.5	8.44
6	8.3	6.8	9.2	8.8	6.0	11.5
7	7.9	6.0	7.8	7.2	6.2	11.1
8	8.2	6.4	8.8	7.4	5.8	8.02
9	8.1	10.6	13.9	11.2	6.2	12.2
10	8.0	7.6	13.1	8.2	3.3	10.6
11	8.2	8.8	20.7	7.1	5.8	22.7
12	8.4	6.5	16.4	5.9	5.6	20.4
13	8.1	7.6	9.6	8.6	5.9	10.8
14	7.9	8.0	9.6	8.4	6.6	10.0
15	8.4	7.2	13.0	7.6	3.7	9.4
16	8.2	7.1	9.4	6.7	6.7	6.9
17	8.4	6.2	16.0	6.0	6.2	13.1
18	8.1	7.1	14.9	6.4	7.1	12.7
19	8.2	8.4	18.7	7.5	6.9	12.4
20	8.3	7.5	15.1	8.0	8.2	11.1
21	8.0	8.8	11.9	8.6	7.0	8.6
22	8.1	8.5	9.6	7.9	8.5	7.2
23	8.3	5.3	10.7	5.8	4.0	5.5
24	8.0	10.9	15.5	10.0	9.1	12.0
25	8.3	6.9	8.7	5.8	6.7	7.4
26	8.1	8.2	14.7	7.5	7.8	12.0
27	8.2	7.8	15.6	7.5	8.0	10.9
28	8.4	5.7	9.4	5.2	5.2	5.7
29	8.5	12.0	16.2	10.9	9.3	13.5
	8.2	7.6	13.2	7.6	6.3	12.1

Beijbom, O. Domain adaptations for computer vision applications. *arXiv preprint arXiv:1211.4860*, 2012.

Blitzer, J., Dredze, M., and Pereira, F. Biographies, Bollywood, boom-boxes and blenders: Domain adaptation for sentiment classification. In *ACL*, volume 7, pp. 440–447, 2007.

der Maaten, L. Van and Hinton, G. Visualizing data using t-SNE. *Journal of Machine Learning Research*, 9(2579-2605):85, 2008.

Glorot, X., Bordes, A., and Bengio, Y. Domain adaptation for large-scale sentiment classification: A deep learning approach. In *Proceedings of the 28th International Conference on Machine Learning (ICML-11)*, pp. 513–520, 2011.

Gretton, A., Smola, A., Huang, J., Schmittfull, M., Borgwardt, K., and Schölkopf, B. Covariate shift by kernel mean matching. *Dataset shift in machine learning*, 3(4): 5, 2009.

Jiang, J. and Zhai, C. Instance weighting for domain adaptation in NLP. In *ACL*, volume 7, pp. 264–271, 2007.

Markley, F. L. Attitude determination using vector observations and the singular value decomposition. *The Journal of the Astronautical Sciences*, 36(3):245–258, 1988.

Mohri, M. Adaptation based on generalized discrepancy. *Journal of Machine Learning Research*, 2015.

Pan, S. J., Tsang, I. W., Kwok, J. T., and Yang, Q. Domain adaptation via transfer component analysis. *Neural Networks, IEEE Transactions on*, 22(2):199–210, 2011.

Patel, V. M., Gopalan, R., Li, R., and Chellappa, R. Visual domain adaptation: A survey of recent advances. *Signal Processing Magazine, IEEE*, 32(3):53–69, 2015.

Xue, Y., Liao, X., Carin, L., and Krishnapuram, B. Multi-task learning for classification with Dirichlet process priors. *Journal of Machine Learning Research*, 8:35–63, 2007.